Sea surface temperature retrieval from landsat8 thermal infrared remote sensing data in coastal waters

Sea surface temperature retrieval from landsat8 thermal infrared remote sensing data in coastal waters

Jiaoqi Fu[1], Chao Chen[1,] *, Huazhong Ren[2], Yuhuan Zhang[3], and Yanli Chu[4]

[1]Marine Science and Technology College, Zhejiang Ocean University, Zhoushan, PR China

[2]Institute of Remote Sensing and GIS, Peking University, Beijing 100871, PR China

[3]Ministry of Ecology and Environment Center for Satellite Application on Ecology and Environment, Beijing 100094, PR China

[4]School of Port and Transportation Engineering, Zhejiang Ocean University, Zhoushan, PR China

* Corresponding author: Chao Chen, chenchao@zjou.edu.cn

Abstract. Since the launch of landsat8, high-quality surface observation data have been acquired. But the corresponding sea surface temperature (SST) products have not been seen. Moreover, the existing SST inversion algorithm do not carefully consider the effect of water vapor on the accuracy. In this study, a new method is proposed for the retrieve of SST from Landsat 8 Thermal Infrared Remote Sensing (TIRS) data based on the variation of atmospheric water vapor content. The steps are briefly described as follows: 1) constructing the SST retrieval model of thermal infrared remote sensing by using the radiation transfer equation with atmospheric profile data (air temperature and pressure); 2) retrieving SST of Zhoushan sea area, China from Landsat 8 TIRS Data; 3) evaluating the accuracy of proposed model by simulation data and AVHRR SST product. The bias and RMSE based on the simulation data are within 0.4 K. The bias and RMSE based on AVHRR SST product are 1.6063 K and 1.8507 K, respectively. The results show that the accurate SST with high spatial resolution could be obtained by using the method.

1. Introduction

Sea surface temperature (SST) is an important parameter to describe air-sea interaction and the state of marine structure. It plays an important role in marine monitoring, numerical prediction, seasonal forecasting of marine and atmospheric system and climate change monitoring [1]. Due to the large heat capacity of seawater, a small variation of ocean temperature will impact on local or even global weather and change the human living environment [2]. Therefore, studying on SST is not only of great scientific value, but also of great significance to human activities and social economy.

In recent years, the application of satellite remote sensing technology in SST observation has become common [3]. According to relevant research, thermal infrared remote sensing has a capability on the inversion of SST in land-sea interaction area and offshore area. In this study, a method is proposed to retrieve SST in coastal waters with thermal infrared remote sensing dataset collected from Landsat-8 Thermal Infrared Sensor (TIRS). It is of great significance to the acquisition of marine structural parameters, the exploitation of marine resources and the monitoring of marine disasters. In

addition, atmospheric water vapor has a significant attenuation effect on thermal infrared information, which will reduce the accuracy of SST inversion. Therefore, the effect of atmospheric water vapor content on SST is also considered in this study.

2. Research area and data

2.1 Research area

The Zhoushan sea area is located in the north-eastern Zhejiang province, near the East China Sea and Hangzhou Bay, as shown in Fig. 1. It is an open seaport and passageway for the Yangtze River Basin and the Yangtze River Delta.

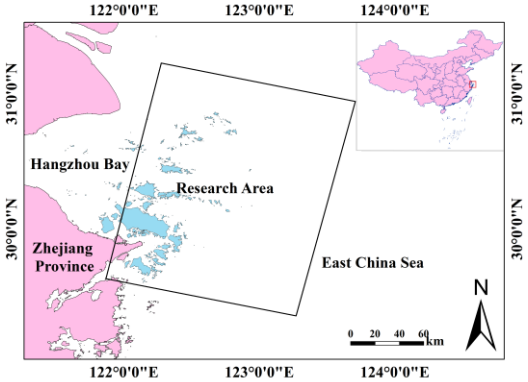

Fig. 1. A sketch map of the research area.

2.2 Data

The atmospheric profile data provided by National Centers for Environmental Prediction (NCEP) was used in this study. NCEP freely provides 17-layer global atmospheric parameter profile at 00:00, 06:00, 12:00 and 18:00 every day since 1948. The spatial resolution is 2.5°×2.5°. The atmospheric pressures of 17-layer are 1000, 925, 850, 700, 600, 500, 400, 300, 250, 200, 150, 100, 70, 50, 30, 20 and 10 hPa, respectively.

In our study, Landsat 8 TIRS data is used to retrieve the offshore SST, with 100m spatial resolution, 15° viewing angle, and 16-day revisit period. Landsat 8 is launched by NASA at Feb. 11th, 2018. It is mainly equipped with Operational Land Imager (OLI) and Thermal Infrared Sensor (TIRS). It has two thermal infrared channels with 10-12micron wavelength. Therefore, Landsat8 satellite is more advantageous than previous series of satellites in SST retrieval [4].

AVHRR is a scanning radiometer with five spectral channels, which was launched and is maintained by National Oceanic and Atmospheric Administration (NOAA). The AVHRR SST data set is obtained by the NOAA National Centers for Environmental Information (NCEI). It provides twice-daily (Day and Night) global SST Level 3 data with a 0.25º×0.25º rectangular grid.

Table 1. Data source.

Data	Information		
	Time	Spatial resolution	Application
NCEP atmospheric profile data	2013.1.1-2018.12.31	2.5°×2.5°	Simulated atmospheric conditions
Landsat8 TIRS data	2015.4.22	100 m	Inversion of SST
AVHRR SST product	2015.4.22	0.25º×0.25º	Model validation

3. Research methods

In our study, a new method is proposed for the retrieve of SST based on the characteristics of Landsat 8 thermal infrared sensor. The detailed research plan is shown as Fig. 2. and described as follows,

1) According to the atmospheric condition simulated by MODTRAN, bright temperature dataset is calculated from radiation transfer equation and Planck's Law. Furthermore, the offshore SST retrieval model could be constructed.

2) SST is retrieved from Landsat-8 TIRS images in coastal waters with the application of the offshore SST retrieval model.

3) The accuracy of derived result is evaluated with simulation data and other satellite SST products.

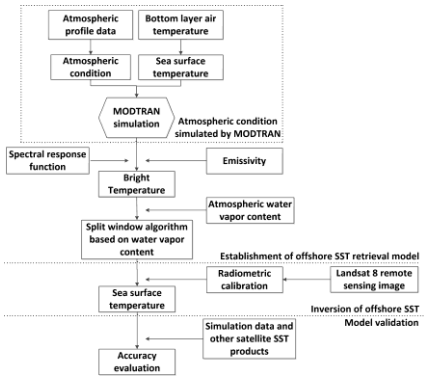

Fig. 2. Technical flow chart.

3.1 Establishment of offshore SST retrieval model

3.1.1 Atmospheric condition simulated by MODTRAN

The radiation signal received by thermal infrared remote sensors consist of three parts: sea surface radiation after atmospheric attenuation, upward atmospheric radiation, downward atmospheric radiation reflected by sea surface. The expression is described as follow [5]:

$$B_i(T_i) = \varepsilon_i B(T_S)\tau_i + R_{atmi}^{\uparrow} + (1-\varepsilon_i) R_{atmi}^{\downarrow}\tau_i \qquad (1)$$

where B_i is the Planck function; T_i is the bright temperature observed at the top of atmosphere in channel i; T_S is sea surface temperature; ε_i is offshore seawater emissivity; τ_i is atmospheric transmittance; $R_{atmi}^{\uparrow}$ and $R_{atmi}^{\downarrow}$ are the upward atmospheric radiation and downward atmospheric radiation, respectively.

In order to retrieve the SST accurately, the effect of atmosphere on spectral radiation has to be eliminated [6]. In this study, the NCEP atmospheric profile at 12:00 in the period from 2013.1.1 to 2018.12.31 in the Zhoushan sea area was extracted, totalling 2,191. Fig. 3. shows the atmospheric water vapor content and the bottom layer (1000hpa) air temperature for these atmospheric profiles. The atmospheric water vapor content is mainly distributed between 1 g/cm^2 and 5.5 g/cm^2, among which the most is between 1.5 g/cm^2 and 3.5 g/cm^2. The bottom layer air temperature is mainly between 285-301 K, and is concentrated between 290- 299 K.

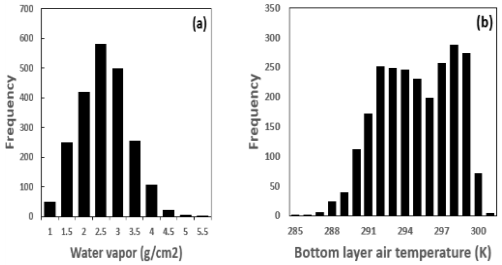

Fig. 3. The distribution of water vapor content and bottom layer air temperature of NCEP atmospheric profiles.

In our study, the bottom layer air temperature is regarded as SST. The upward atmospheric radiation $R_{atmi}^{\uparrow}$, downward atmospheric radiation $R_{atmi}^{\downarrow}$ and atmospheric transmittance τ_i are simulated by the atmospheric radiation transfer software MODTRAN with the atmospheric profiles mentioned above [7]. The results are shown in Fig. 4. In generally, the main components of atmosphere are concentrated in the lower atmosphere. This situation will result in upward radiation less than downward radiation. In addition, the atmospheric radiation of channel 11 is mostly larger than that of channel 10, and the transmittance of channel 11 is less than that of the channel 10.

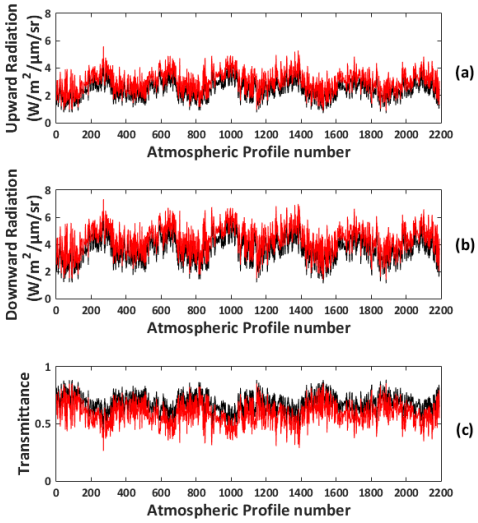

Fig. 4. The upward atmospheric radiation (a), downward atmospheric radiation (b) and atmospheric transmittance (c) of the two thermal infrared channels simulated by MODTRAN. Black is channel 10, red is channel 11.

3.1.2 Bright temperature calculated by Planck's Law

Planck imported quantum theory to blackbody radiation source. It successfully gives the distribution function of blackbody radiation energy varied with wavelength in theory, and called Planck's Law. The expression is described as follow [8],

$$B(\lambda,T)=\frac{2\pi hc^2}{\lambda^5}\left(e^{\frac{hc}{k\lambda T}}-1\right)^{-1} \qquad (2)$$

where the unit of $B(\lambda,T)$ W/(m^2·μm); c represents light speed; h = 6.6262×10^{-34} J·S, is Planck constant; k = 1.3806×10^{-23} J/K, is Boltzmann constant; the unit of wavelength λ and temperature T are μm and K, respectively.

According to the bottom layer air temperature T_0 of each profile, the SST was set into 8 levels, T_S=T_0 + [-10, -5, 0, 5, 10, 15, 20, 25] K. In addition, three seawater emissivity curves were selected from UCSB emissivity database for simulation. Based on eight SST levels, three emissivity samples and the upward atmospheric radiation, downward atmospheric radiation and atmospheric transmittance of the two channels, the radiance in 52,584 cases were simulated by using the radiation transfer equation (Equation 1). Then, the bright temperature observed at the top of atmosphere can be calculated by Planck's law (Equation 2).

3.1.3 The split-window algorithm based on water vapor content

Atmospheric water vapor has obvious attenuation effect on thermal infrared information, which will reduce the inversion accuracy of SST. Therefore, atmospheric water vapor content is added as a variable into the algorithm. Based on the principle of split-window algorithm, a new model is constructed to retrieve SST from brightness temperature T_{i1} and T_{i2} of two thermal infrared channels [8, 9],

$$SST = a_0 + a_1 \cdot T_{i1} + a_2 \cdot T_{i2} + a_3 \cdot (T_{i1} - T_{i2})^2 + a_4 \cdot w + a_5 \cdot w^2 \quad (3)$$

where a_k (k = 0, 1…5) are coefficients; T_{i1} and T_{i2} are the brightness temperature in two thermal infrared channels; SST is the sea surface temperature.

Based on the brightness temperature data of the two channels, the SST and the atmospheric water vapor content, the coefficients a_k were obtained by regression analysis according to equation 3. The result is shown in table 2.

Table 2. The split-window algorithm coefficients obtained by regression analysis.

a_0	a_1	a_2	a_3	a_4	a_5
-0.469	4.006	-3.001	0.037	-0.317	0.089

3.2 Inversion of offshore SST

Generally, the Landsat 8 remote sensing images acquired by users are gray-scale value without physical meaning. Thus, radiometric calibration, which converts gray-scale value into radiance with physical significance, is necessary to performed on the images according to the parameters of the file. In this study, a remote sensing image of Zhoushan sea area on April 22, 2015 was selected for the inversion of SST, as shown in Fig. 5. The SST is retrieved by the radiance information of thermal infrared bands based on the new SST retrieval model. The result of the inversion was shown in Fig. 6.

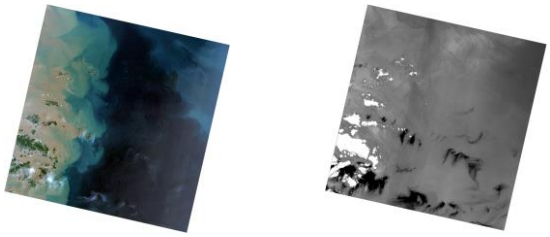

(a) (b)

Fig. 5. The landsat8 image of Zhoushan sea area, China. (a) The true color image, and (b) The thermal infrared image.

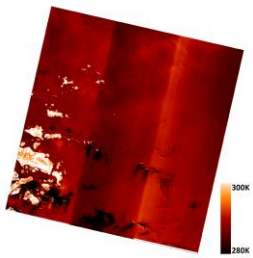

Fig. 6. The SST inversion results.

3.3 Model validation

Accuracy evaluation is indispensable in temperature retrieval. It is not only a standard for evaluating the quality of the method and the influence on the subsequent application, but also an important basis for evaluating the performance of method, adjusting model parameters and optimizing the extraction process [10]. In this section, the accuracy of derived result is evaluated from the simulation data and AVHRR SST products, in order to verify the validity and applicability of the SST retrieval model in coastal waters.

3.3.1 Validation based on simulation data

The observation data is usually used for accuracy evaluation. However, in the absence of observation data, the accuracy of derived result can also be verified by simulation data [11]. In this study, the parameters which obtained during modelling are substituted into the SST retrieval model to calculated

the SST. The accuracy of the proposed algorithm is verified by comparing the initial SST with the inversion SST. The result is shown in Fig. 7(a). The derived result has an average bias of 0.0054 K and a root mean square error (RMSE) of 0.399025 K. The accuracy of the algorithm is good in theory.

3.3.2 Validation based on AVHRR SST products

AVHRR SST products were used to analyze the accuracy of derived result. Although AVHRR SST products cannot fully represent SST, it can be used as an indirect indicator for the accuracy of the inversion results. Fig. 7(b). shows the comparison between the AVHRR SST and the inversion SST. Overall, the inversion results of most checkpoints are about 1 K higher. The derived result has a minimum bias of -0.0517 K, a maximum bias of 3.04177 K, an average bias of 1.6063 K and an RMSE of 1.8507 K. The error is within acceptable range.

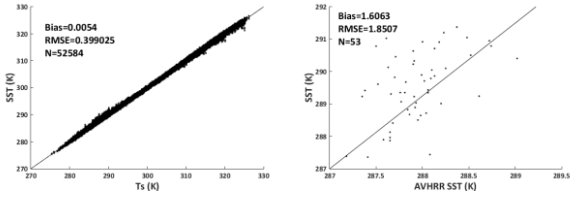

(a) (b)

Fig. 7. Scatterplots for model validation. (a) the initial SST (Ts) and the inversion SST, and (b) the AVHRR SST and the inversion SST (SST).

4. Conclusions

This study proposed a new split-window algorithm considering the variation of atmospheric water vapor content based on Landsat8 TIRS data. The SST inversion and verification were carried out with Zhoushan sea area as the research area. First, the SST retrieval model is established by water vapor content, based on atmospheric correction with MODTRAN. And the Landsat8 remote sensing image was used to retrieve SST. Then, the accuracy of the algorithm was evaluated using simulation data. Both bias and RMSE are within 0.4 K, indicating that the error of the algorithm is small. Finally, AVHRR SST products are used to verify the inversion SST. The bias is 1.6063 K and the RMSE is 1.8507 K. The error of the algorithm is within an acceptable range.

Although some achievements have been made, the following deficiencies still exist in this study. Firstly, in this study, we did not find the observation data of Zhoushan sea area for model validation. The result of accuracy evaluation is not accurate enough to comprehensively analyze the accuracy of the inversion results. Therefore, the observation data and more satellite SST products can be selected to verify the accuracy of the algorithm in the follow-up research works of this study. In addition, combined with the effect of suspended sediment on emissivity, the inversion of offshore SST needs to requires further study.

Acknowledgments

We would like to thank the anonymous reviewers for their constructive comments and suggestions. This work was supported by the National Natural Science Foundation of China (41701447), the Training Program of Excellent Master Thesis of Zhejiang Ocean University.

References

[1] P. J. Minnett, O. B. Brown, R. H. Evans, International Geoscience & Remote Sensing Symposium, (2004)
[2] R. Varelaa, X. Costoyab, C. Enriquezc, F. Santosab, M. Gómez-Gesteira, Journal of Marine Systems **182**, 46-55 (2018)
[3] Y.H. Zhang, H.Y. Chen, Y.J. Chen, Spacecraft Recovery & Remote Sensing **36**, 96-104 (2015)
[4] K. Tan, Z.H. Liao, P. Du and L.X. Wu, Frontiers of Earth Science **11**, 20–34 (2017)

[5] P. Guillevic, J.P. Gastellu, J. Demarty, and L. Preot, Journal of Geophysical Research **108**, 4248 (2003)
[6] Q.G. Xing, C.G. Chen and P. Shi, Acta Oceanologica Sinica **29**, 23-30 (2007)
[7] A. Berk, G.P. Anderson, P.K. Acharya, M.L. Hoke, J.H. Chetwynd, L.S. Bernstein, E.P. Shettle and M.W. Matthew, Air Force Research Lab. Hanscom AFB, (2003)
[8] C. Du, H. Ren, Q. Qin, and J. Meng, Remote Sensing **7**, 647-665 (2015)
[9] G.C. Hulley, S.J. Hook, and P. Schneider, Remote Sensing of Environment **115**, 3758-3769 (2011)
[10] D.L. Jiang, H.H. Kuang, X.F. Cao, Y. Huang, F.R. Li, Remote Sensing Technology and Application **30**, 448-454 (2015)
[11] X.C. Meng, H. Li, Y.M. Du, B. Cao, Q.H. Liu, B. Li, Journal of Remote Sensing **22**, 857-871 (201